ORIGINAL ARTICLE

Potential Diagnostic and Prognostic Role of Microenvironment in Malignant Pleural Mesothelioma

Iris C. Salaroglio, PhD,[a] Joanna Kopecka, PhD,[a] Francesca Napoli, PhD,[b] Monica Pradotto, PhD,[c] Francesca Maletta, MD,[a,d] Lorena Costardi, MD,[e] Matteo Gagliasso, MD,[f] Vladan Milosevic, PhD,[a] Preeta Ananthanarayanan, MSc,[a] Paolo Bironzo, MD, PhD,[a,c] Fabrizio Tabbò, MD,[a,c] Carlotta F. Cartia, MD,[f] Erika Passone, MD,[e] Valentina Comunanza, PhD,[a,g] Francesco Ardissone, MD,[f] Enrico Ruffini, MD,[e] Federico Bussolino, MD, PhD,[a,g] Luisella Righi, MD, PhD,[a,b] Silvia Novello, MD, PhD,[a,c] Massimo Di Maio, MD,[a,h] Mauro Papotti, MD,[a,d] Giorgio V. Scagliotti, MD,[a,c] Chiara Riganti, MD[a,i,*]

[a]*Department of Oncology, University of Torino, Torino, Italy*
[b]*Pathology Unit, Department of Oncology at San Luigi Hospital, University of Torino, Orbassano, Italy*
[c]*Thoracic Oncology Unit and Medical Oncology Division, Department of Oncology at San Luigi Hospital, University of Torino Regione Gonzole 10, Orbassano, Italy*
[d]*Pathology Unit, Department of Oncology at AOU Città della Salute e della Scienza, Torino, Italy*
[e]*Thoracic Surgery Unit, Department of Surgery, AOU Città della Salute e Della Scienza, University of Torino, Torino, Italy*
[f]*Thoracic Surgery Unit, Department of Oncology at San Luigi Hospital, University of Torino, Orbassano, Italy*
[g]*Candiolo Cancer Institute - FPO IRCCS, Candiolo, Department of Oncology, University of Torino, Candiolo, Italy*
[h]*Medical Oncology Division, Department of Oncology at AOU Ordine Mauriziano di Torino, Torino, Italy*
[i]*Interdepartmental Center "G. Scansetti" for the Study of Asbestos and Other Toxic Particulates, University of Torino, Torino, Italy*

Received 21 November 2018; revised 12 March 2019; accepted 31 March 2019
Available online - 9 May 2019

ABSTRACT

Introduction: A comprehensive analysis of the immune cell infiltrate collected from pleural fluid and from biopsy specimens of malignant pleural mesothelioma (MPM) may contribute to understanding the immune-evasion mechanisms related to tumor progression, aiding in differential diagnosis and potential prognostic stratification. Until now such approach has not routinely been verified.

Methods: We enrolled 275 patients with an initial clinical diagnosis of pleural effusion. Specimens of pleural fluids and pleural biopsy samples used for the pathologic diagnosis and the immune phenotype analyses were blindly investigated by multiparametric flow cytometry. The results were analyzed using the Kruskal-Wallis test. The Kaplan-Meier and log-rank tests were used to correlate immune phenotype data with patients' outcome.

Results: The cutoffs of intratumor T-regulatory (>1.1%) cells, M2-macrophages (>36%), granulocytic and monocytic myeloid-derived suppressor cells (MDSC; >5.1% and 4.2%, respectively), CD4 molecule–positive ($CD4^+$) programmed death 1–positive ($PD\text{-}1^+$) (>5.2%) and $CD8^+PD\text{-}1^+$ (6.4%) cells, $CD4^+$ lymphocyte activating 3–positive ($LAG\text{-}3^+$) (>2.8%) and $CD8^+LAG\text{-}3^+$ (>2.8%) cells, $CD4^+$ T cell immunoglobulin and mucin domain 3–positive ($TIM\text{-}3^+$) (>2.5%), and $CD8^+TIM\text{-}3^+$ (>2.6%) cells discriminated MPM from pleuritis with 100% sensitivity and 89% specificity. The presence of intratumor MDSC contributed to the anergy of tumor-infiltrating lymphocytes.

*Corresponding author.

Drs. Salaroglio and Kopecka contributed equally.

Disclosure: Dr. Novello has received has received personal fees from Astra Zeneca, BI, Roche, Pfizer, MSD, Eli Lilly, AbbVie, and Celgene. Dr. Scagliotti has received personal fees from Astra Zeneca, Roche, Pfizer, MSD, Eli Lilly, AbbVie; and has received support from MSD and Bayer. The remaining authors declare no conflict of interest.

Address for correspondence: Chiara Riganti, MD, Department of Oncology, University of Torino, via Santena 5/bis, 10126, Torino, Italy.
E-mail: chiara.riganti@unito.it

ISSN: 1556-0864
https://doi.org/10.1016/j.jtho.2019.03.029

The immune phenotype of pleural fluid cells had no prognostic significance. By contrast, the intratumor T-regulatory and MDSC levels significantly correlated with progression-free and overall survival, the PD-1$^+$/LAG-3$^+$/TIM-3$^+$ CD4$^+$ tumor-infiltrating lymphocytes correlated with overall survival.

Conclusions: A clear immune signature of pleural fluids and tissues of MPM patients may contribute to better predict patients' outcome.

Keywords: Malignant pleural mesothelioma; Tumor-infiltrating lymphocytes; T-regulatory cells; Myeloid-derived suppressor cells; Immune checkpoints

Introduction

Malignant pleural mesothelioma (MPM) is an asbestos-related cancer characterized by a long latency.[1] It has a low mutational burden and the tumor microenvironment rather than the genetic abnormalities in mesothelial cells may contribute to MPM development and progression.[2] The MPM microenvironment is rich of immunosuppressive and anergic immune cells, such as T-regulatory (Treg), granulocytic, and monocytic myeloid-derived suppressor cells (Gr-MDSC/Mo-MDSC) and M2-polarized tumor associated macrophages (TAMs), that — together with soluble factors, such as cytokines, chemokines, and kynurenine, the product of 2,3-indoleamine dioxygenase enzyme — lead to a poor response to immune therapy.[3-9]

Several cytokines accumulated in the pleural effusion of MPM patients promote the M2 polarization of macrophages.[10,11] M2/M3-macrophages and Gr-MDSC of MPM patients, as well as MPM cells reduce the proliferation of heterologous CD8a molecule–positive (CD8$^+$) T lymphocytes, by producing immunosuppressive mediators such as reactive oxygen species (ROS), nitric oxide (NO) and kynurenine.[3,4,7,10,12-14] MDSCs are killed by active CD8$^+$ T lymphocytes, whereas either Tregs and MDSCs reduce CD8$^+$ T lymphocyte activity and memory CD8$^+$ T lymphocyte recruitment, inducing a vicious immunosuppressive circle.[4,6,15-18]

The high expression of immune checkpoints on T lymphocytes and of their ligands on MPM cell has another crucial role in the MPM-induced anergy of tumor-infiltrating lymphocytes (TILs).[5] The programmed death 1 (PD-1)/programmed death ligand 1 (PD-L1) axis is the more extensively studied and the most correlated with early progression and shorter survival.[3,19-23] Lymphocyte activating 3 (LAG-3) and T cell immunoglobulin and mucin domain 3 (TIM-3) have been detected on CD4$^+$ and CD8$^+$ TILs or in formalin-fixed paraffin embedded samples.[24,25] Despite the high interpatient and intrasample variability, both LAG-3 and TIM-3 contribute to the functional exhaustion of TILs.[26] Furthermore, cytotoxic T-lymphocyte associated protein 4 (CTLA-4) has been investigated as a potential therapeutic target in MPM, but the CTLA-4 inhibitor Tremelimumab did not show higher efficacy than placebo in a double blind phase II trial, raising concerns about the role of this immune checkpoint in MPM-induced immunosuppression.[27]

The dissection of the immunoenvironment of MPM is difficult and has often twisted conflicting findings for different reasons. For instance, the number of T cells and macrophages detected in pleural effusion does not always mirror the amount of the same cells infiltrating MPM tissue.[28] Some studies reported the same immunosignature in the MPM pleural effusion and in the peripheral blood, whereas others did not, raising concerns about peripheral blood as a biologic surrogate that reliably reproduces the MPM immunoenvironment.[4,24] Immune cells can be continuously exchanged between pleural cavity and tumor tissue, and/or between peripheral blood and pleural environment. This dynamic immunoenvironment leads to an inhomogeneous distribution of immune cells within MPM tissue. Moreover, the immunoenvironment is exposed to time changes related to the natural tumor progression and/or to chemotherapy-related effects.[28] Also, qualitative and quantitative changes in tumor/stroma ratio may produce a dramatic rewiring in the MPM-infiltrating immune cell subsets.[17] The high intrapatient variability, the intratumor heterogeneity, and the different timing of analysis may partially justify the divergent results.[29]

A simultaneous analysis of all the immunopopulations detectable in the pleural effusion and infiltrating the tissue has never been performed. The present study aims at a comprehensive analysis of the immune infiltrate detected in the pleural fluid and in the biopsy specimens of pleural tissue collected during routine diagnostic procedures from patients with pleural effusions of unknown origin to identify an immune phenotype with diagnostic and prognostic value in MPM patients.

Materials and Methods

Samples Collection

From June 2016 through June 2018 we enrolled 275 patients with an initial clinical diagnosis of pleural effusion of unknown origin. The enrollment of patients was stopped when we reached the sample size with an

adequate power in the MPM patient cohort (see "Statistical analysis" below). Samples were obtained during diagnostic thoracostomies at the Thoracic Surgery Division of San Luigi Gonzaga Hospital, Orbassano, Italy, and AOU Città della Salute e della Scienza, Torino, Italy. Two aliquots of pleural fluid and pleural tissue were collected by thoracic surgeons at the same time for each patient. Each sample was managed by the pathology unit of the two institutions: one aliquot was used for diagnostic purposes according to local pathology guidelines; the second one was used for the research study here reported. In case of limited volume of pleural fluid or limited dimension of pleural tissue, both aliquots were dedicated to the diagnostic workup. In accordance with this criterion, 183 pleural fluids and 119 pleural biopsy specimens were available for the research study. Within all these samples there were 63 pathologically diagnosed nonmalignant pleuritis, 49 MPMs, and 32 pleural metastases (MTS) of malignant tumors for pleural fluid; 16 nonmalignant pleuritis samples, 33 MPMs, and 5 MTS for pleural tissue biopsy specimens met the technical inclusion criteria (see Phenotyping of Immune Cells) and were analyzed in this study. Nine patients who were with pathologically diagnosed with pleuritis and 20 patients who were pathologically diagnosed with MPM had both pleural fluid and pleural tissue available for the study. The flow chart of sample collection and processing is reported in Supplementry Figure 1. The characteristics of samples used for the immunophenotyping in the present study are reported in Supplementary Table 1. The anonymized patients' history (asbestos exposure and smoking status, whenever available), the pathologic diagnosis, and the clinical follow-up (progression-free survival [PFS] and overall survival [OS]) of MPM patients who were treated at the Thoracic Oncology Unit, San Luigi Gonzaga Hospital, are reported in Supplementary Table 2. All patients with MPM were in advanced clinical stage and all were treated with standard cytotoxic chemotherapy according to current guidelines.[30] Researchers performing the immunophenotyping analyses reported below worked in a blind manner, being unaware of the pathologic diagnosis at the time of the assays. The pathologic diagnosis and immunophenotype analysis was performed during the final data analysis. The Ethics Committee of San Luigi Gonzaga Hospital, Orbassano, Italy, approved the study (#126/2016).

Sample Processing and Mesothelial/Tumor Histologic Analysis

Fifty milliliters of pleural fluid were centrifuged at 1200 × g for 5 minutes, washed in phosphate-buffered saline (PBS) containing 1 mg/mL ciprofloxacin (Sigma Chemicals Co., St. Louis, Missouri), and resuspended at 1×10^6 cells/mL in Ham's F10 nutrient mixture medium (Invitrogen Life Technology, Milano, Italy), supplemented with 10% v/v fetal bovine serum (FBS; Sigma Chemicals Co.), 1% v/v penicillin-streptomycin (Sigma Chemicals Co.). Tissues were digested in medium containing 1 mg/mL collagenase and 0.2 mg/mL hyaluronidase (Sigma Chemicals Co.) for 1 hour at 37°C. Cells from pleural fluid and digested tissue were seeded in culture flasks (Becton Dickinson, Franklin Lakes, New Jersey) for 24 hours in complete medium. After this period, the cells floating in the supernatant, that is, immune cells in the pleural fluid or infiltrating the tissue, were collected, counted, and analyzed for their immunophenotype as detailed below. Adherent cells were analyzed for their mesothelial/tumor origin: after detaching by gentle scraping, cells were centrifuged at 1200 × g for 5 minutes, fixed in 4% v/v formalin at 4°C overnight and stained with the following antibodies: calretinin (Thermo Fisher Scientific, Waltham, Massachusetts), Wilms tumor-1 antigen (Thermo Fisher Scientific), cytokeratin 5 (Menarini Diagnostics, Bagno a Ripoli, Italy), podoplanin (Dako, Santa Clara, California), pancytokeratin (Dako), epithelial membrane antigen (Dako), carcinoembrionic antigen (Dako), using an automated immunostainer (Benchmark Ventana Medical Systems, Tucson, Arizona).

Phenotyping of Immune Cells

From all the samples available for research purpose, only samples with 1×10^6 or more viable (i.e., Trypan-blue–negative) cells in the supernatants or adherent in flask were included in the analysis. Preliminary set-up experiments indicated that greater than or equal to 1×10^6 viable cells was the minimal number required allowing to acquire 1×10^5 cells/staining to perform the whole set of the immunophenotyping tests on each sample. Samples with less than or equal to 1×10^6 viable cells were excluded because they did not allow to acquire 1×10^5 cells/staining. The supernatants were centrifuged at 1200 × g for 5 minutes, and the pellet was washed in PBS and resuspended in PBS containing 5% v/v FBS. A three- and four-color flow cytometry was performed, with the appropriate combinations of antibodies (all diluted 1:10, from Miltenyi Biotec, Teterow, Germany, if not otherwise specified) against: CD3 (mouse clone REA613), CD4 (mouse clone M-T466), and CD8 (mouse clone BW135/80) for T lymphocytes; CD25 (mouse clone 4E3) and CD127 (mouse clone MB1518C9) for Treg cells; CD56 (mouse clone AF127H3) and CD335/NKp46 (mouse clone 9E2) for natural killer (NK) cells; CD19 (mouse clone REA675) for B lymphocytes; CD14 (mouse clone TÜK4) and CD68 (mouse clone Y1/

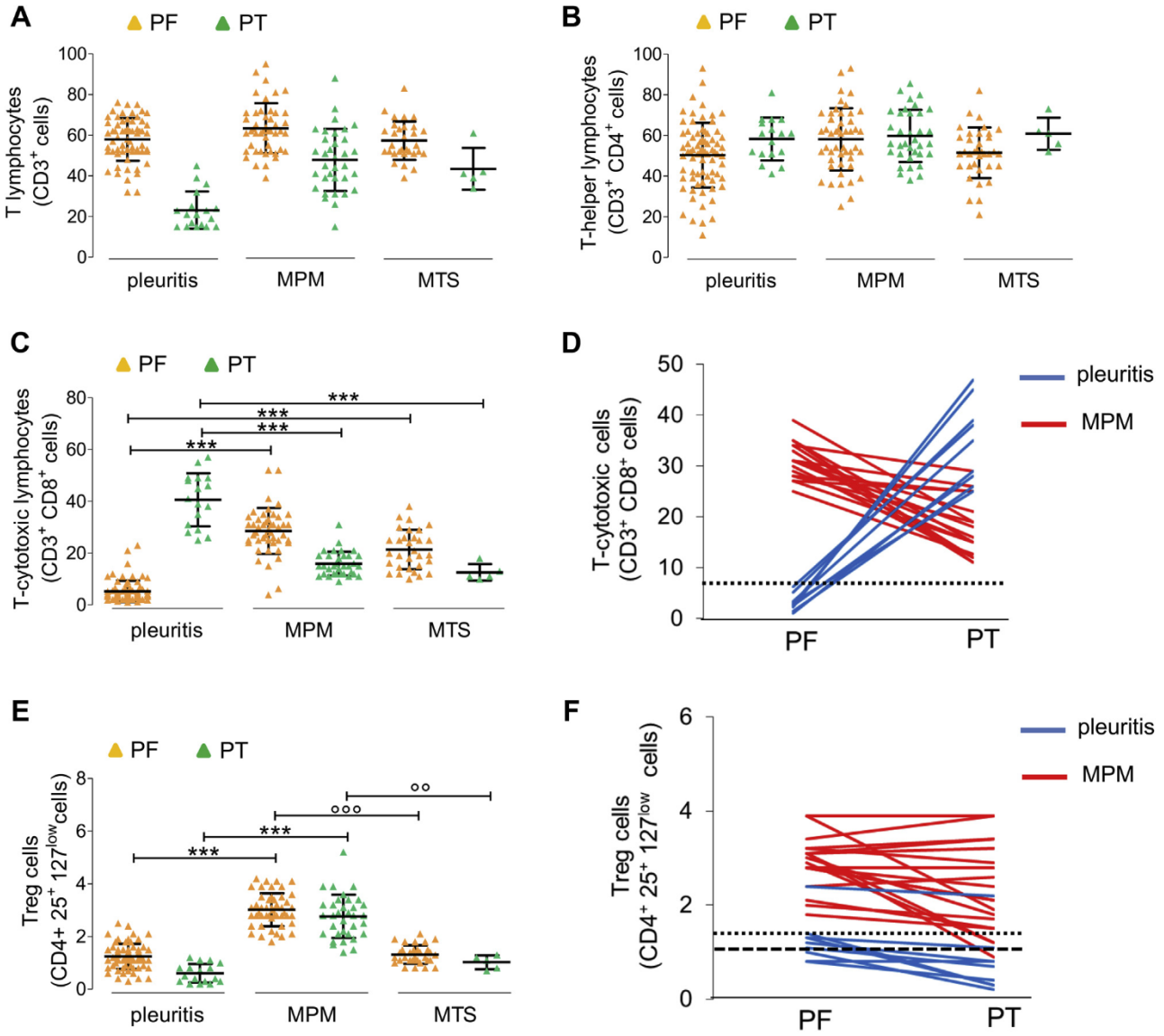

Figure 1. Lymphocyte subtypes present in pleural fluid (PF) and tissue of malignant pleural mesothelioma (MPM). Cells collected from PF of patients with pleuritis (n = 63), MPM (n = 49), and other tumors metastasizing (MTS) to pleura (n = 32), and from digested pleural tissue (PT) of patients with pleuritis (n = 16), MPM (n = 33), and MTS (n = 5) were analyzed by flow cytometry. In nine 9 cases and 20 MPM cases, PF and PT from the same patients were analyzed in parallel. (*A-C*) Percentage of total ($CD3^+$), T-helper ($CD3^+CD4^+$), and T-cytotoxic ($CD3^+CD8^+$) lymphocytes. Data are presented as mean ± SD. Values of 25th percentile, median, 75th percentile: (*A*) pleuritis PF: 52.00, 61.00, and 66.00; pleuritis PT: 15.00, 21.00, and 26.75; MPM PF: 52.00, 62.00, and 71.00; MPM PT: 37.75, 47.00, and 58.75; MTS PF: 51.00, 55.00, and 64.00; MTS PT: 36.50, 41.00, and 51.50 ;(*B*) pleuritis PF: 39.25, 52.00, and 60.50; pleuritis PT: 51.00, 61.00, and 67.00; MPM PF: 48.25, 61.00, and 70.25; MPM PT: 51.00, 56.00, and 71.00; MTS PF: 45.10, 51.50, and 60.50; MTS PT: 54.00, 61.00, and 67.50; and (*C*) pleuritis PF: 2.90, 3.75, and 5.98; pleuritis PT: 30.00, 41.00, and 49.00; MPM PF: 25.00, 29.00, and 33.00; MPM PT: 12.00, 15.00, and 19.00; MTS PF: 14.50, 20.00, and 26.00; MTS PT: 10.50, 11.00, and 15.50. ***$p < 0.001$: MPM/MTS vs. pleuritis; not significant: MPM vs MTS. (*D*) Disaggregated data of T-cytotoxic cells percentage in PF and PT from the same patient. Dotted line: 6.3% cutoff value in PF (false-negative: 0%; false-positive: 0%; sensitivity: 100%; specificity: 100%). (*E*) Percentage of T-regulatory (Treg; $CD4^+$ $CD25^+CD127^{low}$) cells. Data are presented as mean ± SD. Values of 25th percentile, median, 75th percentile: pleuritis PF: 0.90, 1.20, and 1.50; pleuritis PT: 0.30, 0.50, and 0.90; MPM PF: 2.73, 2.95, and 3.48; MPM PT: 2.10, 2.80, and 3.25; MTS PF: 1.10, 1.25, and 1.50; MTS PT: 0.75, 1.10, and 1.25. ***$p < 0.001$: MPM vs. pleuritis; °°$p < 0.005$, °°°$p < 0.001$: MPM vs. MTS. (*F*) Disaggregated data of Treg cells percentage in PF and PT from the same patient. *Dotted line*: 1.4% cutoff value in PF; *dashed line*: 1.1% cutoff value in PT (false-negative: 0%; false-positive: 11%; sensitivity: 100%; specificity: 89%).

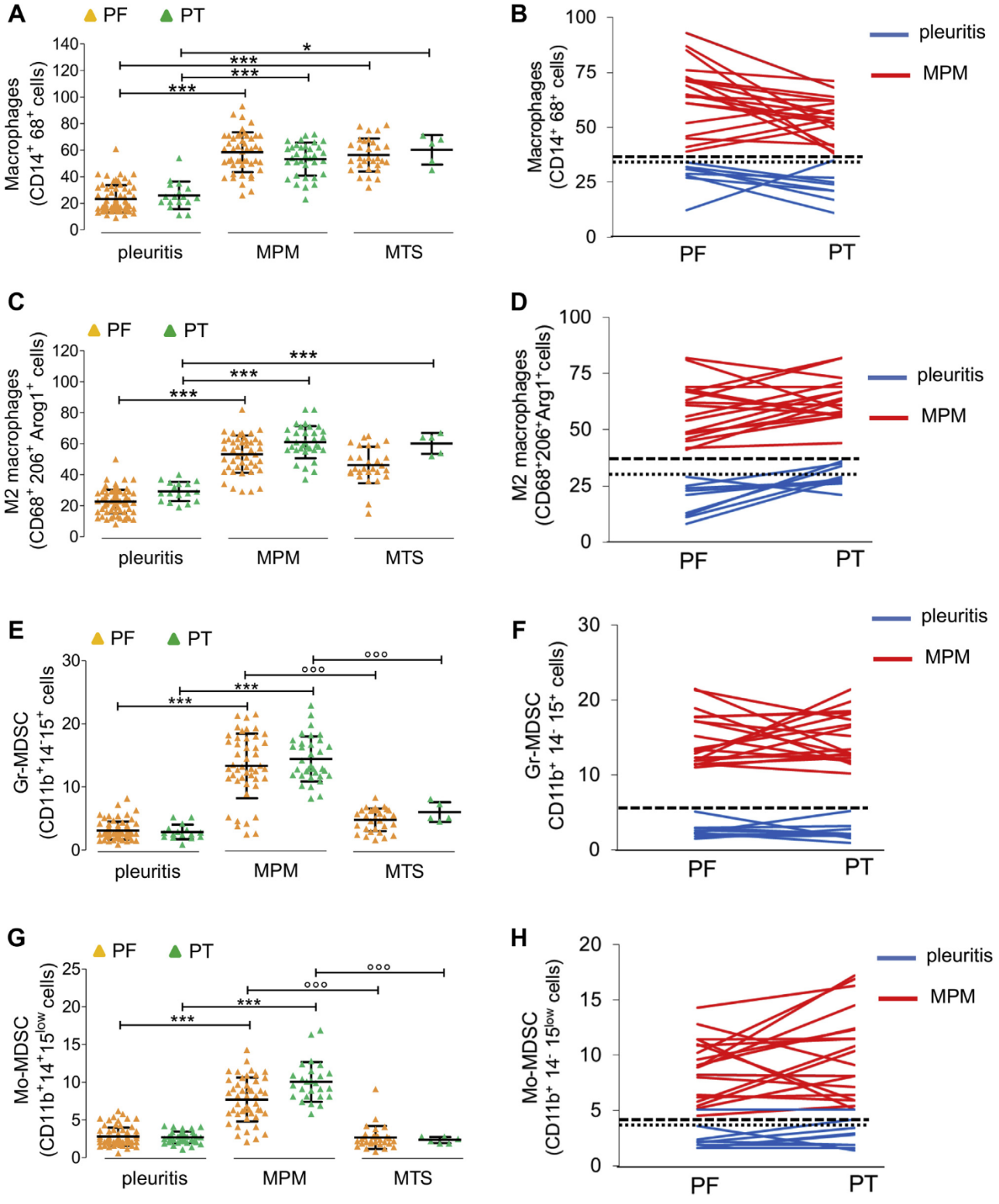

Figure 2. Macrophage and myeloid-derived suppressor cell subtypes present in pleural fluid (PF) and pleural tissue (PT) of malignant pleural mesothelioma (MPM). Cells collected from PF of patients with pleuritis (n = 63), MPM (n = 49) and other tumors metastasizing (MTS) to pleura (n = 32), and from digested PT of patients with pleuritis (n = 16), MPM (n = 33), and MTS (n = 5) were analyzed by flow cytometry. In 9 pleuritis cases and 20 MPM cases, PF and PT from the same patients were analyzed in parallel. (*A*) Percentage of macrophages ($CD14^{+}CD68^{+}$ cells). Data are presented as mean ± SD. Values of 25th percentile, median, 75th percentile: pleuritis PF: 15.00, 19.00, and 31.00; pleuritis PT: 21.00, 25.00, and 32.00; MPM PF: 49.25, 61.00, and 71.00; MPM PT: 41.75, 55.00, and 62.25; MTS PF: 48.25, 54.00, and 66.25; MTS PT: 48.50, 65.00, and 69.50.

82A) for monocytes and macrophages; CD68 (mouse clone Y1/82A), CD208 (mouse clone DCN228), and Arginase-1 (sheep polyclonal, # IC5868A, R&D Biosystems; Minneapolis, Minnesota) for M2-polarized macrophages; CD68 (mouse clone Y1/82A), CD86 (mouse, clone FM95), and iNOS (rabbit polyclonal, #SPC-1325, StressMark Biosciences Inc., Victoria, Canada) for M1-polarized macrophages; CD11b (rat clone M1/70.15.11.5), CD14 (mouse clone TÜK4), and CD15 (mouse clone VIMC6) for Gr-MSDCs and Mo-MDSCs. In each combination staining, 1×10^5 cells were analyzed using a Guava easyCyte flow cytometer (Millipore, Bedford, Massachusetts), equipped with the InCyte software.

Expression of Immune Checkpoints and Immune Checkpoint Ligands

$CD3^+$ cells were isolated from 1×10^6 immune cells of the supernatant of each culture with the Pan T Cell Isolation Kit (Miltenyi Biotec), washed, and resuspended in PBS containing 5% v/v FBS. The detection of immune checkpoints on $CD3^+$ T lymphocytes and/or immune checkpoint ligands on MPM cells were performed using antibodies for CD279/PD-1 (mouse clone PD1.3.1.3), CD223/LAG-3 (clone REA351), CD366/TIM-3 (mouse clone F38-2E2), CD152/CTLA-4 (mouse clone BNI3; all diluted 1:10, Miltenyi Biotec), CD274/PD-1L (1:100, mouse clone 29E.2A3, BioLegend, San Diego, California), and anti-GAL-9 (mouse, clone 9M1-3, BioLegend). In each combination staining 1×10^5 cells were analyzed using a Guava EasyCyte flow cytometer equipped with the InCyte software.

MDSC Functional Properties

ROS were measured using the fluorescent probe 5-(and-6)-chloromethyl-2′,7′-dichlorodihydro-fluorescein diacetate-acetoxymethyl ester (DCFDA-AM), as previously reported.[31] The levels of nitrite, the stable derivative of NO, in cell culture supernatants were measured by the Griess method.[32] The amount of kynurenine was assessed by spectrophotometry.[33] The results were expressed as nmole/mg cellular proteins.

Proliferation and Activation of T Lymphocytes Co-Cultured With MDSC

Sorted intratissue Gr-MDSCs and Mo-MDSCs (1×10^4) were co-cultured for 6 days at a 1:1 ratio with sorted intratissue $CD3^+CD8^+$ T-cytotoxic lymphocytes, either autologous or heterologous, as detailed in the experimental section, in the presence of anti-CD3/anti-CD28 dynabeads (Invitrogen Life Technologies) to activate lymphocytes. The proliferation of T lymphocytes was assessed by adding 1 μCi of [^{3}H]thymidine (PerkinElmer, Waltham, Massachusetts) for 18 hours before the end of the co-cultures, then harvesting the plates and counting the radioactivity by liquid scintillation count. The results were expressed as count per minute (cpm). The percentage of $CD8^+CD107a^+$ and the production of interferon-γ (IFN-γ), considered indexes of activated cytotoxic T lymphocytes, were measured by flow cytometry and enzyme-linked immunosorbent assay, as reported.[13]

Statistical Analysis

Before enrolling patients, the requested number of patients in the MPM cohort was calculated using G*Power Software (www.gpower.hhu.de) with the following assumptions: significance level (α error probability) less than or equal to 0.05 (power, 1-β error probability = 0.80, effect size $\rho = 0.40$). With these parameters, the sample size required was 34 ± 2 MPMs.

The normality distribution of each parameter analyzed was checked with the D'Agostino and Pearson

*$p < 0.01$, ***$p < 0.001$: MPM/MTS vs. pleuritis. (*B*) Disaggregated data of macrophage percentage in PF and PT from the same patient. *Dotted line*: 34% cutoff value in PF, *dashed line*: 35% cutoff value in PT (false-negative: 0%; false-positive: 0%; sensitivity: 100%; specificity: 100%). (*C*) Percentage of M2-macrophages ($CD68^+CD206^+Arg1^+$ cells). Data are presented as mean ± SD. Values of 25th percentile, median, 75th percentile: pleuritis PF: 17.25, 22.00, and 28.00; pleuritis PT: 23.00, 28.00, and 34.50; MPM PF: 45.00, 55.00, and 62.25; MPM PT: 56.00, 60.00, and 68.25; MTS PF: 41.25, 44.00, and 57.00; MTS PT: 53.00, 64.00, and 65.00. ***$p < 0.001$: MPM/MTS vs. pleuritis. (*D*) Disaggregated data of M2-macrophage percentage in PF and PT from the same patient. *Dotted line*: 29% cutoff value in PF, *dashed line*: 36% cutoff value in PT (false-negative: 0%; false-positive: 0%; sensitivity: 100%; specificity: 100%). (*E*) Percentage of granulocytic myeloid-derived suppressor cells (Gr-MDSC; $CD11b^+CD14^-CD15^+$cells). Data are presented as mean ± SD. Values of 25th percentile, median, 75th percentile: pleuritis PF: 2.20, 2.80, and 3.68; pleuritis PT: 2.10, 2.60, and 3.10; MPM PF: 11.23, 13.05, and 17.73; MPM PT: 11.80, 13.15, and 17.03; MTS PF: 3.28, 5.15, and 6.30; MTS PT: 4.80, 5.10, and 7.70. ***$p < 0.001$: MPM vs. pleuritis; °°°$p < 0.001$: MPM vs. MTS. (*F*) Disaggregated data of Gr-MDSC percentage in PF and PT from the same patient. *Dashed line*: 5.1% cutoff value in PF and PT (false-negative: 0%; false-positive: 0%; sensitivity: 100%; specificity: 100%). (*G*) Percentage of monocytic myeloid-derived suppressor cells (Mo-MDSC; $CD11b^+CD14^+CD15^{low}$ cells). Data are presented as mean ± SD. ***$p < 0.001$: MPM vs. pleuritis; °°°$p < 0.001$: MPM vs. MTS. Values of 25th percentile, median, 75th percentile: pleuritis PF: 2.10, 2.40, and 3.45; pleuritis PT: 2.13, 2.75, and 3.18; MPM PF: 5.90, 8.20, and 10.20; MPM PT: 8.10, 9.75, and 11.28; MTS PF: 1.30, 2.30, and 2.90; MTS PT: 1.90, 2.35, and 2.80. (*H*) Disaggregated data of Mo-MDSC percentage in PF and PT from the same patient. *Dotted line*: 3.6% cutoff value in PF, *dashed line*: 4.2% cutoff value in PT (false-negative: 0%; false-positive: 11%; sensitivity: 100%; specificity: 89%).

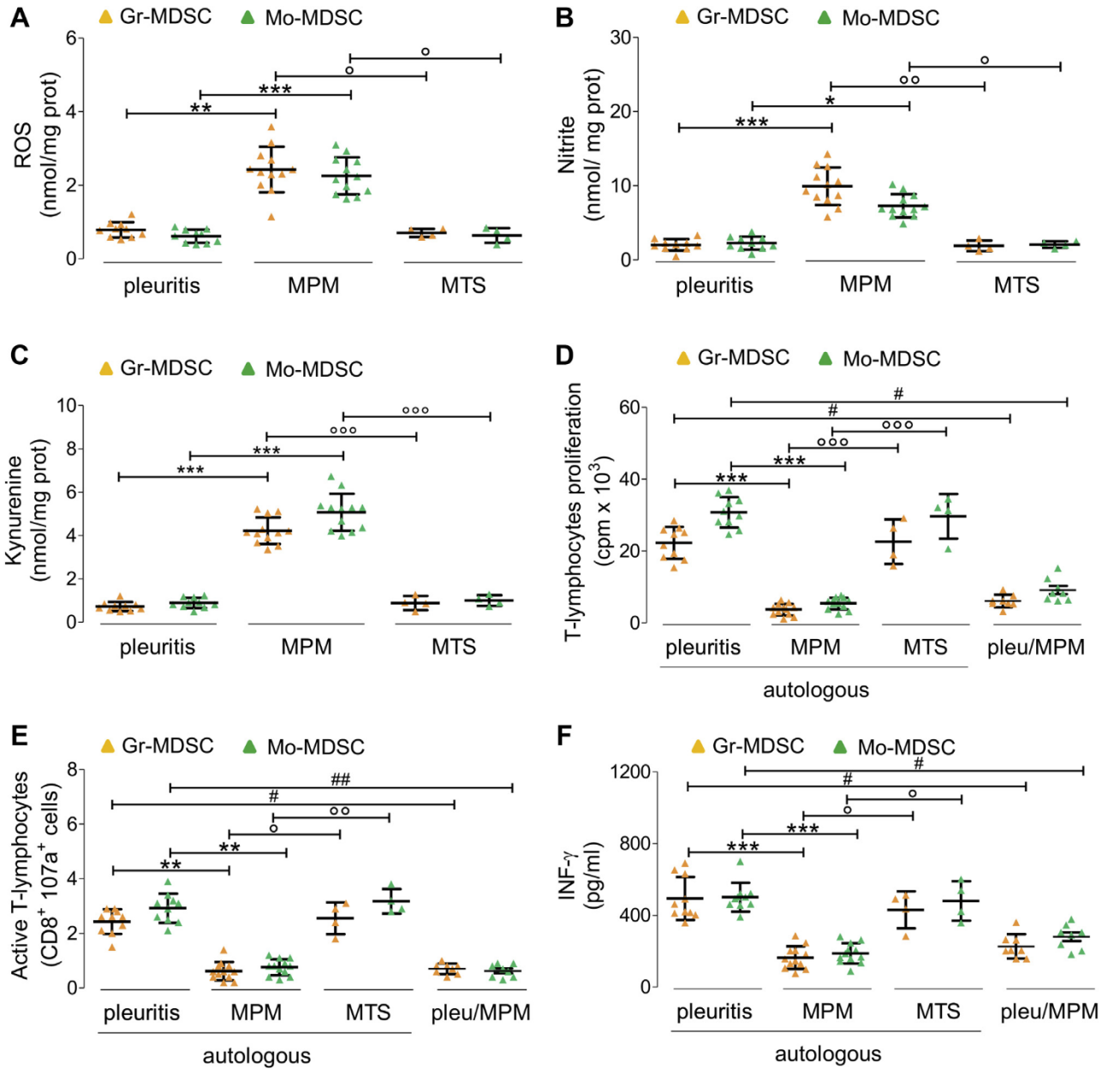

Figure 3. Intratumor myeloid-derived suppressor cells determines $CD8^+$ T-lymphocytes anergy. Sorted (1×10^4) intratissue granulocyte myeloid-derived suppressor cells (Gr-MDSCs) and monocytic-MDSCs (Mo-MDSCs) derived from pleuritis (n = 10), MPM (n = 12), and other tumors metastasizing (MTS) to pleura (n = 4) were seeded and analyzed after 24 hours (*A-C*), or co-cultured (*D-F*) for 6 days with the sorted intratissue $CD3^+CD8^+$ T-cytotoxic lymphocytes of the corresponding patient (autologous setting). When indicated, Gr-MDSCs and Mo-MDSCs from MPM patients were cultured with T-cytotoxic lymphocytes from pleuritis patients (pleu/MPM setting; n = 8). (*A-C*) Intracellular ROS (*A*) were measured fluorimetrically, nitrite (*B*) and kynurenine (*C*) released in the supernatants were measured spectrophotometrically. Data are presented as mean ± SD. Values of 25th percentile, median, 75th percentile: (*A*) pleuritis Gr-MDSC: 0.59 0.79, and 0.94; pleuritis Mo-MDSC: 0.43, 0.65, and 0.80; MPM Gr-MDSC: 2.08, 2.40, and 2.78; MPM Mo-MDSC: 1.78, 2.20, and 2.68; MTS Gr-MDSC: 0.61, 0.72, and 0.81; MTS Mo-MDSC: 0.43, 0.66, and 0.82; (*B*) pleuritis Gr-MDSC: 1.58, 2.00, and 2.45; pleuritis Mo-MDSC: 1.60, 2.10, and 2.95; MPM Gr-MDSC: 8.20, 9.75, and 12.25; MPM Mo-MDSC: 6.05, 6.85, and 8.55; MTS Gr-MDSC: 1.30, 1.75, and 2.65; MTS Mo-MDSC: 1.63, 2.15, and 2.45; (*C*) pleuritis Gr-MDSC: 0.55, 0.72, and 0.82; pleuritis Mo-MDSC: 0.72, 0.87, and 1.16; MPM Gr-MDSC: 3.73, 4.14, and 4.85; MPM Mo-MDSC: 4.25, 5.26, and 5.35; MTS Gr-MDSC: 0.59, 0.89, and 1.19; MTS Mo-MDSC: 0.78, 1.00, and 1.24. *$p < 0.01$, **$p < 0.005$, ***$p < 0.001$: MPM vs. pleuritis; °$p < 0.01$, °°$p < 0.005$, °°°$p < 0.001$: MPM vs. MTS. (*D-F*) The proliferation of T-cytotoxic lymphocytes (*D*) was measured radiometrically, the percentage of $CD8^+CD107a^+$ lymphocytes (*E*) was measured by flow cytometry, the amount of interferon- γ (IFN-γ) (*F*) in the supernatants was measured by enzyme-linked immunosorbent assay. The proliferation of T lymphocytes in the absence of anti-CD3/anti-CD28 dynabeads, used as negative control, was less than 3500 cpm for all experimental conditions. Data are presented as mean ± SD. Values of 25th percentile, median, 75th percentile: (*D*) pleuritis Gr-MDSC: 18.09, 23.12, and

test. All parameters had a Gaussian distribution or approximation. However, the results were conservatively analyzed by the nonparametric Kruskal-Wallis test (GraphPad PRISM 6.0 software). All data in the figures are provided as mean ± SD. Medians and quartile values are reported in the figure legends. To partially correct for the multiplicity of tests performed, a conservative p less than 0.01 was considered statistically significant. For each parameter, specific cutoffs discriminating MPM from pleuritis were calculated to have a 100% sensitivity (0% false-negatives) and greater than 89% specificity (<11% false-positives). To correlate the immune parameters with PFS and OS, since there are no previously reported and validated cutoff values for the immune-phenotypic parameters analyzed, patients were exploratively divided into "low expressing" and "highly expressing" groups if their value was below or equal/above the median value, respectively. The Kaplan-Meier method was used to calculate PFS and OS. Log rank test was used to compare the outcome of each group as hazard ratio (i.e., risk of patient death). Considering the exploratory nature of the survival analysis, no adjustment for multiplicity was made, and p less than 0.05 was considered statistically significant.

Results

High Treg Cells/High MDSCs Discriminate MPM From Inflammatory Pleuritis and Secondary Pleural Tumors

$CD3^+$ T lymphocytes represented the prevalent immune population within pleural fluid or pleural tissue, without differences between samples of pleuritis, MPM, or MTS (Fig. 1*A*). $CD3^+CD4^+$ T-helper lymphocytes were up to 60% in all the samples, without differences between patient subgroups (Fig. 1*B*). $CD3^+CD8^+$ T-cytotoxic lymphocytes, representing approximately 5% of immune cells in pleural fluids from pleuritis, significantly increased in MPM and MTS-pleural fluid samples. By contrast they represented up to 50% of TILs in pleuritis and significantly decreased in MPM and MTS (Fig. 1*C*). This trend allowed to discriminate pleuritis (all with $CD3^+CD8^+$ cells < 6.3% in pleural fluid) from MPM (all with $CD3^+CD8^+$ cells > 25% in pleural fluid) (Fig. 1*D*). Treg cells were significantly higher in both pleural fluid and tissue from MPM patients compared to pleuritis and MTS-derived samples (Fig. 1*E*). A cutoff of greater than 1.4% in pleural fluid and greater than 1.1% in pleural tissue Treg cells identified 100% (20 of 20) MPMs and excluded 88.8% (8 of 9) pleuritis cases (Fig. 1*F*). NK and B lymphocytes were poorly represented and did not show any differences among groups (Supplementary Figs 2*A* and *B*).

Also, monocytes did not differ (Supplementary Fig. 3), whereas pleural fluid and tissue macrophages were significantly higher in MPM and MTS-derived samples (Fig. 2*A*). All pleuritic samples had less than 34% macrophages in pleural fluid and less than 35% in tissue, whereas all MPM samples were above these thresholds (Fig. 2*B*). More relevantly, the protumorigenic M2-macrophages were higher in MPM and MTS compared to pleuritis (Fig. 2*C*). According to these parameters, a clear separation between pleuritis (100% of patients with M2-macrophages <29% in pleural fluid and <36% in pleural tissue) and MPM (100% of patients with M2-macrophages >41% in pleural fluid and >44% in pleural tissue) was clearly identified (Fig. 2*D*). Antitumorigenic M1-macrophages were lower in both pleural fluid and tissue of MPM and MTS compared with pleuritis (Supplementary Fig. 4).

A significantly higher number of Gr-MDSCs (Fig. 2*E*) and Mo-MDSCs (Fig. 2*G*) in pleural fluid and tissue was detected in MPM compared to pleuritis and MTS. A clear threshold of 5.1% Gr-MDSCs in both pleural fluid and tissue discriminated 100% pleuritis from 100% MPM (Fig. 2*F*). A cutoff of greater than 3.6% Mo-MDSCs in pleural fluid and greater than 4.2% in pleural tissue identified 100% MPM and excluded 88.8% pleuritis cases (Fig. 2*H*).

The Intratumor Myeloid-Derived Suppressor Cells Determine T Lymphocytes Anergy

The MDSCs isolated from MPM tissue showed increased production of ROS (Fig. 3*A*), NO (Fig. 3*B*), and kynurenine (Fig. 3*C*) compared to those obtained from tissue biopsy specimens from other subgroups. In co-culture with $CD8^+$ T-cytotoxic lymphocytes from the tissue of the same patient, both Gr-MDSCs and Mo-MDSCs derived from MPM reduced $CD8^+$

26.03; pleuritis Mo-MDSC: 27.53, 30.4, and 34.62; MPM Gr-MDSC:2.42, 4.04, and 5.00; MPM Mo-MDSC: 4.03, 5.71, and 6.84; MTS Gr-MDSC: 16.66, 22.69, and 28.46; MTS Mo-MDSC: 23.27, 31.72, and 33.96; pleu/MPM Gr-MDSC: 5.33, 5.80, and 7.19; pleu/MPM Mo-MDSC: 6.44, 8.25, and 11.70; (*E*) pleuritis Gr-MDSC:2.08, 2.60, and 2.83; pleuritis Mo-MDSC: 2.48, 3.00, and 3.25; MPM Gr-MDSC: 0.40, 0.60, and 0.80; MPM Mo-MDSC: 0.45, 0.80, and 1.05; MTS Gr-MDSC: 1.95, 2.65, and 3.05; MTS Mo-MDSC: 2.83, 3.05, and 3.65; pleu/MPM Gr-MDSC: 0.53, 0.75, and 0.80; pleu/MPM Mo-MDSC: 0.40, 0.65, and 0.88; (*F*) pleuritis Gr-MDSC: 409.50, 441, and 636.50; pleuritis Mo-MDSC: 459.80, 497.50, and 521.00; MPM Gr-MDSC: 111.80, 151.00, and 203.30; MPM Mo-MDSC: 147.00, 177.00, and 236.00; MTS Gr-MDSC: 322.00, 463.50, and 506.80; MTS Mo-MDSC: 373.80, 480.00, and 585.50; pleu/MPM Gr-MDSC: 168.80, 204.50, and 263.80; pleu/MPM Mo-MDSC: 209.80, 298.00, and 335.80.$^{**}p < 0.005$, $^{***}p < 0.001$: MPM vs. pleuritis; $^{\circ}p < 0.01$, $^{\circ\circ}p < 0.005$, $^{\circ\circ\circ}p < 0.001$: MPM vs. MTS in autologous settings; $^{\#}p < 0.01$, $^{\#\#\#}p < 0.001$: pleu/MPM setting vs. pleuritis autologous setting.

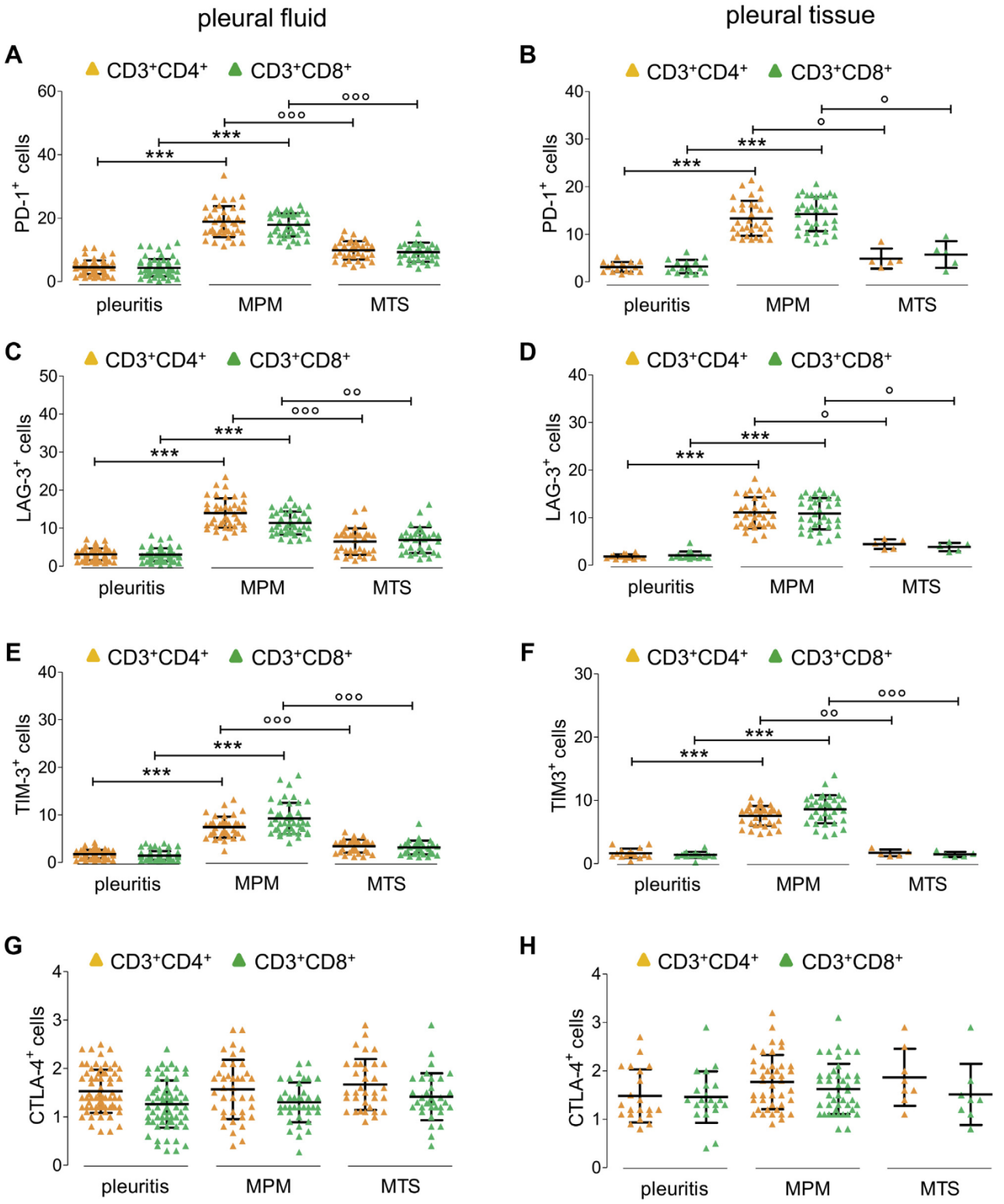

Figure 4. Immune checkpoint expression in T lymphocytes contained in pleural fluid and pleural tissue. Cells collected from pleural fluid of patients with pleuritis (n = 63), malignant pleural mesothelioma (MPM; n = 49) and other tumors metastasizing (MTS) to pleura (n = 32), and from digested pleural tissue of patients with pleuritis (n = 16), MPM (n = 33), and MTS (n = 5) were analyzed by flow cytometry. Data are presented as mean ± SD. (*A*,*B*) Percentage of programed death 1-positive (PD-1$^+$) T-helper ($CD3^+CD4^+$) and T-cytotoxic ($CD3^+CD8^+$) lymphocytes. Values of 25th percentile, median, 75th percentile: (*A*) pleuritis $CD3^+CD4^+$: 2.45, 4.60, and 5.60; pleuritis $CD3^+CD8^+$: 2.50, 3.90, and 5.50; MPM $CD3^+CD4^+$: 15.53, 18.30, and 22.65; MPM $CD3^+CD8^+$: 14.83, 17.65, and 21.38; MTS $CD3^+CD4^+$: 7.95, 10.20, and 12.30; MTS $CD3^+CD8^+$: 7.03, 9.00, and 11.33; (*B*) pleuritis $CD3^+CD4^+$: 2.10, 3.15, and 4.10; pleuritis $CD3^+CD8^+$: 2.03, 2.90, and 4.18;

T lymphocyte proliferation (Fig. 3*D*), CD107a positivity (Fig. 3*E*), and IFN-γ production (Fig. 3*F*), compared to the autologous $CD8^+$ T lymphocytes/MDSCs co-cultures derived from the pleuritis and MTS subgroups. The immunosuppressive properties of both Gr-MDSCs and Mo-MDSCs were further shown by co-incubating Gr-MDSCs and Mo-MDSCs derived from MPM tissue with heterologous T lymphocytes derived from patients with pleuritis. In this setting, proliferation, CD107a positivity, and IFN-γ production of T lymphocytes derived from pleuritis was reduced to the same level of T lymphocytes derived from MPM (Figs. 3*D*, *E* and *F*).

A High Number of Intratumor PD-1$^+$/LAG-3$^+$/TIM-3$^+$ Infiltrating Lymphocytes Is Peculiar for MPM

The immune checkpoints PD-1 (Figs. 4*A* and *B*), LAG-3 (Figs. 4*C* and *D*), and TIM-3 (Figs. 4*E* and *F*) were higher on $CD4^+$ T-helper and $CD8^+$ T-cytotoxic lymphocytes of MPM compared to the lymphocytes from pleuritis and MTS, either in pleural fluid and in pleural tissue. The cutoff values of 6.7% in pleural fluid, 5.2% in pleural tissue for $CD4^+PD1^+$ (Supplementary Fig. 5*A*), 6.3% in pleural fluid, 6.4% in pleural tissue for $CD8^+PD1^+$cells (Supplementary Fig. 5*B*), 4.9% in pleural fluid, 2.8% in pleural tissue for $CD4^+LAG\text{-}3^+$ (Supplementary Fig. 5*C*), 5.2% in pleural fluid, 2.8% in pleural tissue for $CD8^+LAG\text{-}3^+$cells (Supplementary Fig. 5*D*), 1.9% in pleural fluid, 2.5% in pleural tissue for $CD4^+TIM\text{-}3^+$ (Supplementary Fig. 5*E*), 2.4% in pleural fluid, and 2.6% in pleural for $CD8^+TIM\text{-}3^+$cells tissue (Supplementary Fig. 5*F*) discriminated 100% MPM from pleuritis. In our series, the lymphocytic expression of CTLA-4 did not differ between each subgroup (Figs. 4*G* and *H*).

The higher expression of immune checkpoints on T lymphocytes was paralleled by the higher expression of PD-L1 (Fig. 5*A*), LAG-3 (Fig. 5*B*), TIM-3 (Fig. 5*C*), and GAL-9 (Fig. 5*D*) on MPM cells compared to pleuritis and — for LAG-3 and TIM-3 — compared to MTS.

Specific Immune Signatures of Intratumor Infiltrate Have a Prognostic Value

Furthermore, we investigated the potential prognostic role of the immunophenotypic parameters that significantly differed between MPM and pleuritis. The amount of $CD3^+CD8^+$ cells, Treg, M2-polarized macrophages, Gr/Mo-MDSCs, $PD\text{-}1^+/LAG\text{-}3^+/TIM3^+$ $CD4^+$ or $CD8^+$ cells present in the pleural fluids did not show any significant correlation with PFS and OS of MPM patients (Table 1). As far as the intratumor immune infiltrate was concerned, the amount of $CD3^+CD8^+$ cells and M2 were not associated with any prognostic significance, whereas high intratumor Treg, Gr-MDSCs, and Mo-MDSCs significantly correlated with shorter PFS and OS (Table 1; Supplemental Figs 6*A*–*E*). The amount of $PD\text{-}1^+$ and $LAG\text{-}3^+$ $CD4^+$ cells correlated with a lower OS (Table 1; Supplementary Figs. 7*A*–*C*). The expression of immune checkpoints on intratumor $CD8^+$ had no prognostic significance (Table 1; Supplementary Figs. 8*A*–*C*).

Discussion

Specific immunophenotypic markers on tissue microarrays or fine-needle aspirate are currently investigated to better characterize the immune-environment of MPM.[20,24] The present study for the first time assessed a comprehensive and multiparametric analysis of the immune infiltrate of either pleural fluid or pleural tissue, performed in parallel with

MPM $CD3^+CD4^+$: 10.20, 12.50, and 16.15; MPM $CD3^+CD8^+$: 11.28, 15.20, and 18.05; MTS $CD3^+CD4^+$: 3.60, 4.30, and 6.50; MTS $CD3^+CD8^+$: 3.10, 6.20, and 8.15. $^{***}p < 0.001$: MPM vs. pleuritis; $^{\circ}p < 0.01$, $^{\circ\circ\circ}p < 0.001$: MPM vs. MTS. (*C*,*D*) Percentage of lymphocyte activating 3-positive ($LAG\text{-}3^+$) T-helper ($CD3^+CD4^+$) and T-cytotoxic ($CD3^+CD8^+$) lymphocytes. Values of 25th percentile, median, 75th percentile: (*C*) pleuritis $CD3^+CD4^+$: 1.90, 2.80, and 4.15; pleuritis $CD3^+CD8^+$: 1.90, 2.80, and 4.15; MPM $CD3^+CD4^+$: 10.83, 13.35, and 16.25; MPM $CD3^+CD8^+$: 8.83, 10.60, and 14.05; MTS $CD3^+CD4^+$: 3.88, 7.20, and 8.40; MTS $CD3^+CD8^+$: 3.75, 7.15, and 8.60; (*D*) pleuritis $CD3^+CD4^+$: 1.50, 1.85, and 2.10; pleuritis $CD3^+CD8^+$: 1.60, 1.80, and 2.18; MPM $CD3^+CD4^+$: 8.38, 10.50, and 14.28; MPM $CD3^+CD8^+$: 8.10, 10.50, and 14.10; MTS $CD3^+CD4^+$: 3.40, 4.60, and 5.40; MTS $CD3^+CD8^+$: 2.95, 4.10, and 4.65. $^{***}p < 0.001$: MPM vs. pleuritis; $^{\circ}p < 0.01$, $^{\circ\circ}p < 0.005$, $^{\circ\circ\circ}p < 0.001$: MPM vs. MTS. (*E*,*F*) Percentage of hepatitis A virus cellular receptor 2-positive ($TIM\text{-}3^+$) T-helper ($CD3^+CD4^+$) and T-cytotoxic ($CD3^+CD8^+$) lymphocytes. Values of 25th percentile, median, 75th percentile: pleuritis $CD3^+CD4^+$:1, 1.80, 2.48; (*E*) pleuritis $CD3^+CD8^+$: 0.90, 1.35, and 1.70; MPM $CD3^+CD4^+$: 6.10, 7.30, and 8.40; MPM $CD3^+CD8^+$: 6.65, 8.30, and 10.70; MTS $CD3^+CD4^+$: 2.18, 3.85, and 4.43; MTS $CD3^+CD8^+$: 1.98, 3.15, and 4.13; (*F*) pleuritis $CD3^+CD4^+$: 1.13, 1.50, and 2.05; pleuritis $CD3^+CD8^+$: 1.20, 1.35, and 1.58; MPM $CD3^+CD4^+$: 6.18, 8.10, and 8.53; MPM $CD3^+CD8^+$: 6.78, 9.10, and 10.20; MTS $CD3^+CD4^+$: 1.25, 1.60, and 2.20; MTS $CD3^+CD8^+$: 1.15, 1.40, and 1.85. $^{***}p < 0.001$: MPM vs. pleuritis; $^{\circ\circ}p < 0.005$, $^{\circ\circ\circ}p < 0.001$: MPM vs. MTS. (*G*,*H*) Percentage of cytotoxic T-lymphocyte associated protein 4-positive ($CTLA\text{-}4^+$) T-helper ($CD3^+CD4^+$) and T-cytotoxic ($CD3^+CD8^+$) lymphocytes. Values of 25th percentile, median, 75th percentile: (*G*) pleuritis $CD3^+CD4^+$: 1.20, 1.40, and 1.90; pleuritis $CD3^+CD8^+$: 0.90, 1.30, and 1.58; MPM $CD3^+CD4^+$: 1.10, 1.60, and 1.90; MPM $CD3^+CD8^+$: 1.10, 1.20, and 1.50; MTS $CD3^+CD4^+$: 1.18, 1.50, and 2.10; MTS $CD3^+CD8^+$: 1.20, 1.30, and 1.80; (*H*) pleuritis $CD3^+CD4^+$: 1.10, 1.20, and 2.05; pleuritis $CD3^+CD8^+$: 1.25, 1.40, and 1.70; MPM $CD3^+CD4^+$: 1.30, 1.80, and 2.10; MPM $CD3^+CD8^+$: 1.20, 1.50, and 1.90; MTS $CD3^+CD4^+$: 1.45, 1.70, and 2.38; MTS $CD3^+CD8^+$: 1.13, 1.40, and 1.73.

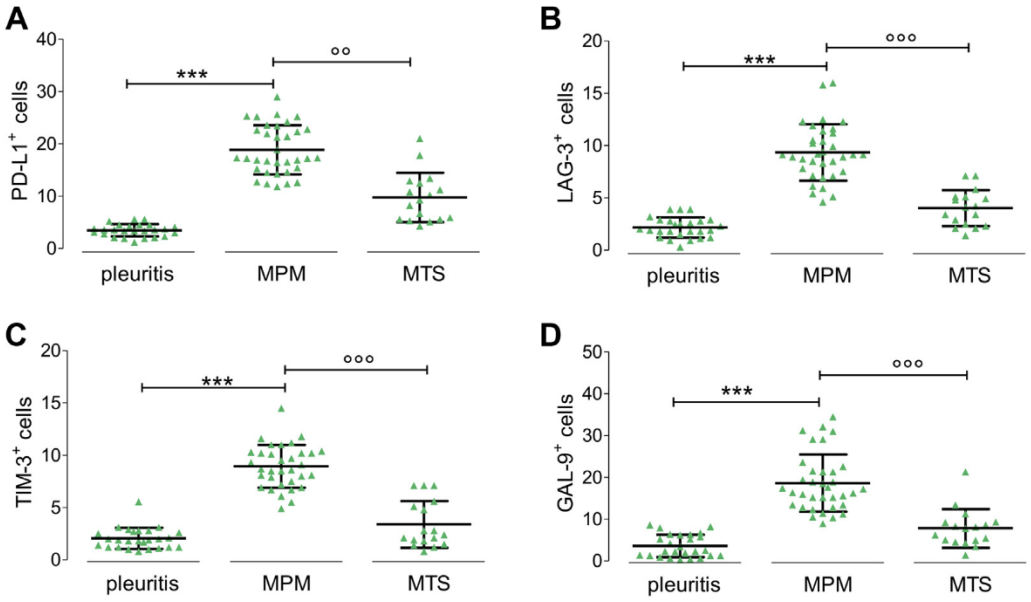

Figure 5. Immune checkpoint ligands expressed in malignant pleural mesothelioma cells. Mesothelial cells collected from patients with pleuritis (n = 24), malignant pleural mesothelioma (MPM) cells (n = 33), or cells from different tumors metastasizing (MTS) to pleura (n = 16), were analyzed by flow cytometry for the expression of programmed death ligand 1 (PD-L1) (*A*), lymphocyte activating 3 (LAG-3) (*B*), hepatitis A virus cellular receptor 2 (TIM-3) (*C*), and GAL-9 (*D*). Data are presented as mean ± SD. Values of 25th percentile, median, 75th percentile: (*A*) pleuritis: 2.55, 3.60, and 4.35; MPM: 15.05, 17.25, and 22.95; MTS: 5.60, 9.30, and 12.70; (*B*) pleuritis: 1.43, 1.95, and 2.83; MPM: 7.40, 9.10, and 11.25; MTS: 2.40, 4.10, and 5.10; (*C*) pleuritis: 1.20, 1.90, and 2.73; MPM: 7.35, 8.70, and 10.25; MTS: 1.65, 2.40, and 5.35; (*D*) pleuritis: 1.30, 2.40, and 6.23; MPM: 13.40, 17.20, and 21.50; MTS: 4.70, 7.80, and 9.25.***$p < 0.001$: MPM vs. pleuritis; °°$p < 0.005$, °°°$p < 0.001$: MPM vs. MTS.

the routine diagnostic procedures. Based on flow cytometry assays, our experimental model allows one to recover viable cells, coupling the phenotypic analysis with functional assays of adaptive immunity. Moreover, we detected a robust immune signature that discriminates MPM from pleuritis and from pleural metastases secondary to other malignancies. By selecting specific cutoffs for each immune parameter analyzed with 100% sensitivity and greater than or equal to 89% good specificity, we maximized the possibility to identify correctly all the MPM patients, accepting the possibility to have sporadic cases of pleuritis erroneously identified as MPM. Because all samples were subjected to the usual pathologic diagnoses, the rare pleuritic cases erroneously identified as MPM on the basis of immunophenotype analysis could be easily re-verified by the pathologist and/or clinically followed-up more strictly. The analysis of the immune parameters was not intended to replace the pathologic diagnosis but simply to complement the pathologic diagnosis of MPM with a set of immunologic tests and potential new prognostic information. Each parameter was correlated with PFS or OS, exploratively using the median values as cutoffs because in literature there were no previously reported and validated cutoffs for the parameters analyzed and the identification of the optimal cutoff was beyond the scope of this analysis.

The first relevant finding discriminating MPM from nonmalignant pleuritis was the higher intrapleural fluid $CD8^+$ T lymphocytes coupled with the lower intrapleural $CD8^+$ TILs. The amount of $CD8^+$ TILs has been associated with adverse or good prognosis, but in our case series, we did not detect any prognostic significance.[17,20,34] It is likely that — more than the absolute number of $CD8^+$ T lymphocytes — their functional exhaustion, due to the presence of Treg cells and MDSCs, is critical in determining tumor progression and patients' outcome.[6,17]

We identified high Treg cells within pleural fluid and tissue as specific biomarkers of MPM rather than of benign pleural disease or pleural MTS. The high amount of intra-MPM Tregs was a negative prognostic factor, whereas the amount of Tregs in pleural fluid had no clinical significance, as reported previously.[17] This data indicated that the intratumor immune-infiltrate — more than the immune population in the pleural effusion — in this case is more reliable in predicting the patients' outcome.

As expected, we did not detect significant differences in overall TAMs between MPM and metastatic patients. Compared to pleuritis, M2-macrophages were increased in both tumor and pleural fluid of MPM. The correlations between the number of TAMs or the ratio M2/TAM and the tumor progression or

Table 1. Survival Analysis According to the Immunophenotypic Parameter Characterizing Mesothelioma Patients

Immune Population	Sample	PFS (mo) (95% CI)	*p* Value	OS (mo) (95% CI)	*p* Value
$CD3^+CD8^+$ low vs. $CD3^+CD8^+$ high	PF	6.3 ± 1.6 vs. 6.3 ± 1.0 (5.0-8.3)	0.913	10.0 ± 2.2 vs. 10.8 ± 1.1 (8.2-12.7)	0.6927
Treg low vs. Treg high	PF	6.0 ± 1.1 vs. 7.0 ± 1.6 (4.7-8.1)	0.496	10.8 ± 1.6 vs. 9.7 ± 1.4 (8.2-12.7)	0.4347
M2 low vs. M2 high	PF	7.0 ± 1.3 vs. 5.7 ± 1.0 (4.7-7.8)	0.2851	10.9 ± 1.5 vs. 9.8 ± 1.9 (8.2-12.7)	0.7424
Gr-MDSC low vs. Gr-MDSC high	PF	7.1 ± 1.1 vs. 5.6 ± 1.3 (4.6-8.1)	0.3351	10.6 ± 1.4 vs. 10.8 ± 2.2 (8.2.9-13.1)	0.4522
Mo-MDSC low vs. Mo-MDSC high	PF	6.8 ± 1.2 vs. 5.9 ± 1.4 (4.4-8.1)	0.8755	10.8 ± 1.6 vs. 9.4 ± 1.7 (7.9-12.5)	0.5498
$CD4^+PD\text{-}1^+$ low vs. $CD4^+PD\text{-}1^+$ high	PF	5.7 ± 1.3 vs. 7.3 ± 1.1 (4.7-8.1)	0.713	8.6 ± 1.5 vs. 12.4 ± 1.6 (8.2-12.7)	0.1126
$CD4^+LAG\text{-}3^+$ low vs. $CD4^+LAG\text{-}3^+$ high	PF	7.2 ± 1.4 vs. 7.3 ± 1.1 (5.0-8.4)	0.4585	9.6 ± 2.5 vs. 10.9 ± 1.1 (8.2-12.7)	0.7886
$CD4^+TIM\text{-}3^+$ low vs. $CD4^+TIM\text{-}3^+$ high	PF	8.1 ± 1.1 vs. 5.0 ± 1.3 (4.9-8.4)	0.1047	11.9 ± 1.2 vs. 9.1 ± 2.1 (8.4-12.9)	0.5417
$CD8^+PD\text{-}1^+$ low vs. $CD8^+PD\text{-}1^+$ high	PF	7.2 ± 1.3 vs. 6.8 ± 1.2 (5.3-8.8)	0.6309	9.4 ± 2.0 vs. 10.0 ± 1.4 (7.6-11.9)	0.9571
$CD8^+LAG\text{-}3^+$ low vs. $CD8^+LAG\text{-}3^+$ high	PF	6.5 ± 1.4 vs. 4.8 ± 0.8 (4.1-7.2)	0.2127	11.0 ± 1.8 vs. 10.1 ± 1.9 (8.1-13.0)	0.8569
$CD8^+TIM\text{-}3^+$ low vs. $CD8^+TIM\text{-}3^+$ high	PF	7.7 ± 1.1 vs. 4.3 ± 1.2 (4.31-7.6)	0.0956	11.0 ± 1.6 vs. 9.7 ± 1.6 (8.2-12.3)	0.5441
$CD3^+CD8^+$ low vs. $CD3^+CD8^+$ high	PT	7.4 ± 1.0 vs. 8.0 ± 1.3 (6.1-9.2)	0.8624	9.6 ± 1.4 vs. 10.3 ± 1.3 (8.3-11.9)	0.9594
Treg low vs. Treg high	PT	9.1 ± 1.8 vs. 4.7 ± 1.4 (6.1-9.3)	**0.0172**	12.1 ± 1.2 vs. 7.6 ± 1.0 (8.3-11.9)	**0.0046**
M2 low vs. M2 high	PT	7.6 ± 1.7 vs. 8.8 ± 1.1 (6.4-10.2)	0.8228	10.4 ± 1.4 vs. 9.3 ± 1.2 (8.1-11.7)	0.4016
Gr-MDSC low vs. Gr-MDSC high	PT	9.1 ± 1.1 vs. 5.6 ± 1.0 (5.9-9.2)	**0.0427**	11.3 ± 1.3 vs. 7.5 ± 1.1 (7.6-11.2)	**0.037**
Mo-MDSC low vs. Mo-MDSC high	PT	11.2 ± 1.2 vs. 7.3 ± 1.4 (7.7-11.5)	**0.0178**	11.1 ± 1.7 vs. 8.0 ± 1.0 (8.1-11.4)	**0.026**
$CD4^+PD\text{-}1^+$ low vs. $CD4^+PD\text{-}1^+$ high	PT	7.9 ± 1.0 vs. 7.9 ± 1.7 (6.2-9.5)	0.6616	11.4 ± 1.1 vs. 8.3 ± 1.1 (8.5-11.8)	**0.043**
$CD4^+LAG\text{-}3^+$ low vs. $CD4^+LAG\text{-}3^+$ high	PT	8.3 ± 1.1 vs. 7.0 ± 1.3 (6.1-9.3)	0.364	11.5 ± 1.4 vs. 8.0 ± 0.9 (8.0-11.5)	**0.0077**
$CD4^+TIM\text{-}3^+$ low vs. $CD4^+TIM\text{-}3^+$ high	PT	6.8 ± 1.6 vs. 8.4 ± 0.9 (6.1-9.4)	0.7595	11.7 ± 1.2 vs. 7.8 ± 1.2 (8.0-11.7)	**0.044**
$CD8^+PD\text{-}1^+$ low vs. $CD8^+PD\text{-}1^+$ high	PT	7.8 ± 1.3 vs. 7.9 ± 1.2 (6.2-9.5)	0.9333	10.3 ± 1.3 vs. 10.0 ± 1.2 (8.4-11.8)	0.9315
$CD8^+LAG\text{-}3^+$ low vs. $CD8^+LAG\text{-}3^+$ high	PT	6.7 ± 1.3 vs. 8.0 ± 1.1 (5.7-9.0)	0.6298	9.7 ± 1.5 vs. 10.6 ± 1.1 (8.3-11.9)	0.9219
$CD8^+TIM\text{-}3^+$ low vs. $CD8^+TIM\text{-}3^+$ high	PT	6.8 ± 1.7 vs. 8.4 ± 0.8 (6.1-9.3)	0.7423	8.5 ± 1.6 vs. 10.6 ± 1.2 (8.0-11.6)	0.574

The median values of $CD3^+CD8^+$ lymphocytes, Treg, M2-macrophages, Gr-MDSC, Mo-MDSC, $CD4^+PD\text{-}1^+$, $CD4^+LAG\text{-}3^+$, $CD4^+TIM\text{-}3^+$, $CD8^+PD\text{-}1^+$, $CD8^+LAG\text{-}3^+$, and $CD8^+TIM\text{-}3^+$ cells was calculated in pleural fluid (PF; n = 49) and pleural tissue (PT; n = 33). Patients were classified as "low" or "high" if the percentage of each population was low or equal/higher than the median value. Progression-free survival (PFS) and overall survival (OS) probability were calculated using the Kaplan-Meier method, and expressed as mean ± SD (mo). Significant values are indicated by bold type. CI, confidence interval; Treg, T-regulatory cells; CD3, CD3d molecule; Gr-MDSC, granulocyte myeloid-derived suppressor cells; Mo-MDSC, monocyte myeloid-derived suppressor cells; PD-1, programmed death 1; LAG-3, lymphocyte activating 3; TIM-3, hepatitis A virus cellular receptor 2.

patients' outcomes are highly discordant.[8,17,20,34] According to our data, M2 percentage is not a significant predictor of patients' outcome but it is an immune marker that highly differentiates MPM from nonmalignant conditions, as Gr-MDSCs and — to a lesser extent — Mo-MDSCs.

In our study, Gr- and Mo-MDSCs abrogated proliferation and cytotoxic activity of autologous TILs and of TILs derived from patients with pleuritis. These data suggest that MDSCs mediate an important role MPM immunosuppression, likely by the increased production of ROS, NO, and kynurenine. Again, only the intratumor-infiltrating MDSCs — and not the MDSCs of pleural fluid — are significantly associated with poorer PFS and OS. Accounting for the dynamic exchange occurring between pleural fluid and tumor, pleural fluid can be considered as a reservoir of immunosuppressive cells[28]: the higher their migration is from pleural fluid into the tumor, the higher the chance is that they characterize an immune-escape status and predict tumor progression.

Immune checkpoint expression is another key player in immunosuppression in MPM. The immunohistochemical expression of PD-L1 and PD-1 is not always reliable as biomarker in discriminating pleuritis from MPM: PD-L1 expression was absent in benign lesions, but PD-1 was expressed more on TILs of nontumoral samples than in TILs of MPM analyzed by immunohistochemistry, a finding contrasting with the high percentage of $PD\text{-}1^+$ cells reported in MPM using flow cytometry.[3,5,19,23] The type of diagnostic antibody and the abundance of the immune infiltrate in the examined sample may explain this discrepancy. The multiparametric flow cytometry analysis revealed that the amount of PD-1 expressed in $CD4^+$ and $CD8^+$ T lymphocytes well discriminates MPM from nonmalignant pleuritis, but not from metastatic cancers, in line with the observation that pleural effusion from lung cancer are also rich with $PD1^+CD8^+$ T lymphocytes and $PD\text{-}L1^+$ cancer cells.[35]

Our data indicate that the expression of PD-1, LAG-3, and TIM-3 in TILs, but not in T cells in pleural effusion, correlated with lower OS. The lack of correlation between immune checkpoint levels and PFS likely suggests that the accumulation of immune checkpoint–positive, anergic lymphocytes occurs at advanced stages in MPM patients and determines prognosis in the terminal stages only. Only $PD\text{-}1^+/LAG\text{-}3^+/TIM\text{-}3^+CD4^+$ cells, but not $CD8^+$ cells, were negative prognostic factors. Because $CD4^+$ T cells are a hub in the engagement of other

immune populations, we may hypothesize that a loss of function of $CD4^+$ T lymphocytes impairs the immune recognition of MPM cells more than a dysfunction in the effector $CD8^+$ T cells, leading to faster progression and reduced survival. Among the immune checkpoints analyzed in MPM patients, CTLA-4 was poorly expressed on the surface of T lymphocytes. This is likely related to the cytosol localization of CTLA-4 and the high recycling rate.[36] Our data must be re-assessed when a staining optimization for intracellular CTLA-4 antigen has been achieved.

In conclusion, we propose a comprehensive multiparametric analysis of several immunologic parameters that define an MPM immune signature, reliably applied to both pleural fluid and tissue routinely collected in standard clinical practice. We are aware that our discriminating cutoff values, although significant, have been obtained in a small patient cohort, and we emphasize that the identification of the optimal cutoff was beyond the scope of this analysis. The parameters are now being validated in a larger prospective study, including discovery and validation cohorts, to improve the specificity of the proposed thresholds and evaluate the possible clinical utility of the immune parameters found. In such ongoing study, refined grouping strategies will be adopted to define more accurately the quantitative values of the immunophenotypic parameters significantly correlated with patient survival and other clinical parameters. Only if the validation study will confirm this pilot experience, the immune biomarkers identified in the present study may be considered as additional parameters to be analyzed — beyond the parameters already adopted to perform MPM diagnosis — in challenging clinical cases.

This study is the first aimed to systematically characterize the immune infiltrate of pleural fluid and tumor derived from the same patient. Our results indicate that the analysis of the intratumor immune infiltrate — better than that of pleural fluid — identifies potential prognostic factors. Given the high interpatient and intrapatient variability observed in MPMs, the larger prospective validation study will also clarify if the qualitative and quantitative differences in the intratumor immune infiltrate may be correlated with specific histologic, cytogenetic, and mutational features. This may contribute to more accurate patient stratification for rational and personalized immunotherapy of MPM.

Acknowledgments

This work was supported by Italian Association for Cancer Research (IG21408 to C.R.); Italian Ministry of University and Research (Future in Research program RBFR12SOQ1 to C.R.; Basic Research Funding Program, FABR2017 to LR and CR); Italian Ministry of Health (GR-2011-02348356 to L.R.; Italian Mesothelioma Network-CCM2012 to G.V.S.), Azienda Ospedaliera "SS. Antonio e Biagio e Cesare Arrigo" to G.V.S. for the research activity "MESOLINE," University of Torino (Intramural Grant 2015 to S.N. and C.R.; Intramural Grant 2016 to L.R.; Intramural Grant 2017 to J.K.); Fondazione Cassa di Risparmio di Torino (2016-2443 to C.R.); and ERA-Net Transcan-2-JTC 2017 (TOPMESO to F.B.). Dr. Salaroglio is a post-doctoral research fellow supported by the Fondazione Franco e Marilisa Caligara for Multidisciplinary Sciences, Torino, Italy. Dr. Milosevic is a PhD fellow of Erasmus Mundus-ERAWEB Action 2 program. Dr. Napoli is a student of the Biomedical Sciences and Oncology PhD program. The funding institutions had no role in the study design, data collection and analysis, or in writing the manuscript. The authors thank Mr. Costanzo Costamagna, Department of Oncology, University of Torino, for the technical assistance.

Supplementary Data

Note: To access the supplementary material accompanying this article, visit the online version of the *Journal of Thoracic Oncology* at www.jto.org and at https://doi.org/10.1016/j.jtho.2019.03.029.

References

1. Remon J, Reguart N, Corral J, Lianes P. Malignant pleural mesothelioma: new hope in the horizon with novel therapeutic strategies. *Cancer Treat Rev*. 2015;41:27–34.
2. Stahel RA, Weder W, Felley-Bosco E, et al. Searching for targets for the systemic therapy of mesothelioma. *Ann Oncol*. 2015;26:1649–1660.
3. Awad MM, Jones RE, Liu H, et al. Cytotoxic T cells in PD-L1-positive malignant pleural mesotheliomas are counterbalanced by distinct immunosuppressive factors. *Cancer Immunol Res*. 2016;4:1038–1048.
4. Khanna S, Graef S, Mussai F, et al. Tumor-derived GM-CSF promotes granulocyte immunosuppression in mesothelioma patients. *Clin Cancer Res*. 2018;24:2859–2872.
5. Marcq E, Pauwels P, van Meerbeeck JP, Smits EL. Targeting immune checkpoints: new opportunity for mesothelioma treatment? *Cancer Treat Rev*. 2015;41:914–924.
6. Hegmans JP, Hemmes A, Hammad H, Boon L, Hoogsteden HC, Lambrecht BN. Mesothelioma environment comprises cytokines and T-regulatory cells that suppress immune responses. *Eur Respir J*. 2006;27:1086–1095.
7. Salaroglio IC, Campia I, Kopecka J, et al. Zoledronic acid overcomes chemoresistance and immunosuppression of malignant mesothelioma. *Oncotarget*. 2015;6:1128–1142.
8. Cornelissen R, Lievense LA, Maat AP, et al. Ratio of intratumoral macrophage phenotypes is a prognostic factor in epithelioid malignant pleural mesothelioma. *PLoS One*. 2014;9:e106742.
9. Aerts JG, Lievense LA, Hoogsteden HC, Hegmans JP. Immunotherapy prospects in the treatment of lung

cancer and mesothelioma. *Transl Lung Cancer Res*. 2014;3:34–45.
10. Lievense LA, Cornelissen R, Bezemer K, Kaijen-Lambers ME, Hegmans JP, Aerts JG. Pleural effusion of patients with malignant mesothelioma induces macrophage-mediated T cell suppression. *J Thorac Oncol*. 2016;11:1755–1764.
11. Chéné AL, d'Almeida S, Blondy T, et al. Pleural effusions from patients with mesothelioma induce recruitment of monocytes and their differentiation into M2 macrophages. *J Thorac Oncol*. 2016;11:1765–1773.
12. Jackaman C, Yeoh TL, Acuil ML, Gardner JK, Nelson DJ. Murine mesothelioma induces locally-proliferating IL-10(+)TNF-α(+)CD206(-)CX3CR1(+) M3 macrophages that can be selectively depleted by chemotherapy or immunotherapy. *Oncoimmunology*. 2016;5:e1173299.
13. Riganti C, Lingua MF, Salaroglio IC, et al. Bromodomain inhibition exerts its therapeutic potential in malignant pleural mesothelioma by promoting immunogenic cell death and changing the tumor immune-environment. *Oncoimmunology*. 2017;7:e1398874.
14. Zhao Y, Wu T, Shao S, Shi B, Zhao Y. Phenotype, development, and biological function of myeloid-derived suppressor cells. *Oncoimmunology*. 2015;5:e1004983.
15. Tan Z, Zhou J, Cheung AK, et al. Vaccine-elicited CD8+ T cells cure mesothelioma by overcoming tumor-induced immunosuppressive environment. *Cancer Res*. 2014;74:6010–6021.
16. Yu Z, Tan Z, Lee BK, et al. Antigen spreading-induced CD8+T cells confer protection against the lethal challenge of wild-type malignant mesothelioma by eliminating myeloid-derived suppressor cells. *Oncotarget*. 2015;6:32426–32438.
17. Ujiie H, Kadota K, Nitadori JI, et al. The tumoral and stromal immune microenvironment in malignant pleural mesothelioma: a comprehensive analysis reveals prognostic immune markers. *Oncoimmunology*. 2015;4, e1009285.
18. Scherpereel A, Grigoriu BD, Noppen M, et al. Defect in recruiting effector memory CD8+ T-cells in malignant pleural effusions compared to normal pleural fluid. *BMC Cancer*. 2013;13:e324.
19. Khanna S, Thomas A, Abate-Daga D, et al. Malignant mesothelioma effusions are infiltrated by CD3(+) T cells highly expressing PD-L1 and the PD-L1(+) tumor cells within these effusions are susceptible to ADCC by the anti-PD-L1 antibody avelumab. *J Thorac Oncol*. 2016;11:1993–2005.
20. Pasello G, Zago G, Lunardi F, et al. Malignant pleural mesothelioma immune microenvironment and checkpoint expression: correlation with clinical-pathological features and intratumor heterogeneity over time. *Ann Oncol*. 2018;29:1258–1265.
21. Patil NS, Righi L, Koeppen H, et al. Molecular and histopathological characterization of the tumor immune microenvironment in advanced stage of malignant pleural mesothelioma. *J Thorac Oncol*. 2018;13:124–133.
22. Cedrés S, Ponce-Aix S, Zugazagoitia J, et al. Analysis of expression of programmed cell death 1 ligand 1 (PD-L1) in malignant pleural mesothelioma (MPM). *PLoS One*. 2015;10, e0121071.
23. Combaz-Lair C, Galateau-Sallé F, McLeer-Florin A, et al. Immune biomarkers PD-1/PD-L1 and TLR3 in malignant pleural mesotheliomas. *Hum Pathol*. 2016;52:9–18.
24. Lizotte PH, Jones RE, Keogh L, et al. Fine needle aspirate flow cytometric phenotyping characterizes immunosuppressive nature of the mesothelioma microenvironment. *Sci Rep*. 2016;6:e31745.
25. Marcq E, Siozopoulou V, De Waele J, et al. Prognostic and predictive aspects of the tumor immune microenvironment and immune checkpoints in malignant pleural mesothelioma. *Oncoimmunology*. 2016;6:e1261241.
26. Marcq E, Waele J, Audenaerde JV, et al. Abundant expression of TIM-3, LAG-3, PD-1 and PD-L1 as immunotherapy checkpoint targets in effusions of mesothelioma patients. *Oncotarget*. 2017;8:89722–89735.
27. Maio M, Scherpereel A, Calabrò L, et al. Tremelimumab as second-line or third-line treatment in relapsed malignant mesothelioma (DETERMINE): a multicentre, international, randomised, double-blind, placebo-controlled phase 2b trial. *Lancet Oncol*. 2017;18:1261–1273.
28. Lievense LA, Bezemer K, Cornelissen R, Kaijen-Lambers ME, Hegmans JP, Aerts JG. Precision immunotherapy; dynamics in the cellular profile of pleural effusions in malignant mesothelioma patients. *Lung Cancer*. 2017;107:36–40.
29. Minnema-Luiting J, Vroman H, Aerts J, Cornelissen R. Heterogeneity in immune cell content in malignant pleural mesothelioma. *Int J Mol Sci*. 2018;19. pii: E1041.
30. Baas P, Fennell D, Kerr KM, et al. Malignant pleural mesothelioma: ESMO Clinical Practice Guidelines for diagnosis, treatment and follow-up. *Ann Oncol*. 2015;26(suppl 5):v31–v39.
31. Riganti C, Gazzano E, Gulino GR, Volante M, Ghigo D, Kopecka J. Two repeated low doses of doxorubicin are more effective than a single high dose against tumors overexpressing P-glycoprotein. *Cancer Lett*. 2015;360:219–226.
32. De Boo S, Kopecka J, Brusa D, et al. iNOS activity is necessary for the cytotoxic and immunogenic effects of doxorubicin in human colon cancer cells. *Mol Cancer*. 2009;8:e108.
33. Campia I, Buondonno I, Castella B, et al. An autocrine cytokine/JAK/STAT-signaling induces kynurenine synthesis in multidrug resistant human cancer cells. *PLoS One*. 2015;10, e0126159.
34. Cornelissen R, Lievense LA, Robertus JL, et al. Intratumoral macrophage phenotype and CD8+ T lymphocytes as potential tools to predict local tumor outgrowth at the intervention site in malignant pleural mesothelioma. *Lung Cancer*. 2015;88:332–337.
35. Prado-Garcia H, Romero-Garcia S, Puerto-Aquino A, Rumbo-Nava U. The PD-L1/PD-1 pathway promotes dysfunction, but not "exhaustion," in tumor-responding T cells from pleural effusions in lung cancer patients. *Cancer Immunol Immunother*. 2017;66:765–776.
36. Valk E, Rudd CE, Schneider H. CTLA-4 trafficking and surface expression. *Trends Immunol*. 2008;29:272–279.